

Rank Optimization for MIMO systems with RIS: Simulation and Measurement

Shengguo Meng, Wankai Tang, Weicong Chen, Jifeng Lan,
Qun Yan Zhou, Yu Han, Xiao Li, and Shi Jin

Abstract—Reconfigurable intelligent surface (RIS) is a promising technology that can reshape the electromagnetic environment in wireless networks, offering various possibilities for enhancing wireless channels. Motivated by this, we investigate the channel optimization for multiple-input multiple-output (MIMO) systems assisted by RIS. In this paper, an efficient RIS optimization method is proposed to enhance the effective rank of the MIMO channel for achievable rate improvement. Numerical results are presented to verify the effectiveness of RIS in improving MIMO channels. Additionally, we construct a 2×2 RIS-assisted MIMO prototype to perform experimental measurements and validate the performance of our proposed algorithm. The results reveal a significant increase in effective rank and achievable rate for the RIS-assisted MIMO channel compared to the MIMO channel without RIS.

Index Terms—Reconfigurable intelligent surface, multiple-input multiple-output, measurement, 6G.

I. INTRODUCTION

IN recent years, the increasing presence of various mobile communication services such as video streaming and online gaming has sparked a significant surge in the need for higher data rates. To meet the growing demands, various technologies have been applied. Among them, multiple-input multiple-output (MIMO) technology stands out as a solution to increase system capacity without the need for additional frequency resources. However, as MIMO is widely deployed, new challenges have arisen. In propagation environments characterized by strong line-of-sight (LoS) path and limited scatterings, the correlation in MIMO channels increases. This phenomenon weakens the multiplexing of MIMO, resulting in a reduced capability to support multiple data streams and subsequently diminishing the performance of communication systems. Therefore, there is an urgent need for innovative solutions to optimize the effective rank of MIMO channels to address these challenges. The advent of reconfigurable intelligent surfaces (RIS), which can be integrated into the channel, offers new opportunities for addressing this problem.

As one of the key potential technologies for the sixth-generation (6G) networks, RIS can dynamically manipulate electromagnetic waves [1]–[5], thus holding the potential to

Shengguo Meng, Wankai Tang, Weicong Chen, Jifeng Lan, Yu Han, Xiao Li, and Shi Jin are with the National Mobile Communications Research Laboratory, Southeast University, Nanjing 210096, China. (e-mail: seumengsg@seu.edu.cn; tangwk@seu.edu.cn; cwc@seu.edu.cn; lanjifeng@seu.edu.cn; hanyu@seu.edu.cn; li_xiao@seu.edu.cn; jinshi@seu.edu.cn).

Qun Yan Zhou is with the State Key Laboratory of Millimeter Waves, Southeast University, Nanjing 210096, China. (e-mail: qyzhou@seu.edu.cn).

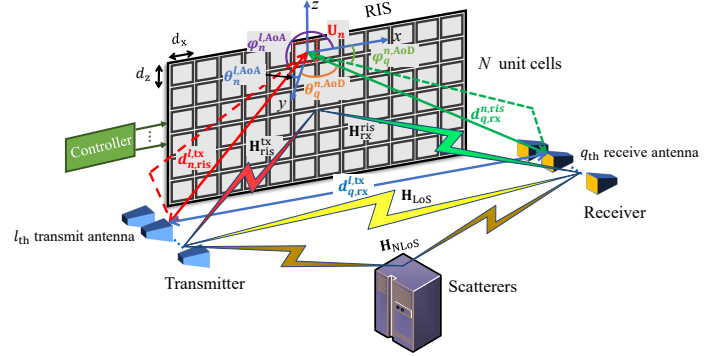


Fig. 1. The considered RIS-assisted MIMO communication system.

customize wireless channels [6]. Some studies have been conducted on leveraging RIS as part of the MIMO channels to improve the achievable rate of the systems [7]–[9]. These related works demonstrate the capability of RIS to improve achievable rates of MIMO systems in different scenarios. Furthermore, RIS can be employed to improve the system performance by directly enhancing the effective rank [10] or minimum singular value of the MIMO channel [11]. However, the optimization algorithms proposed in the aforementioned references are complex and may not be easily applicable to practical systems, rendering a lack of relevant experimental measurements.

In this paper, we first develop an RIS-assisted MIMO channel model and then propose an efficient RIS optimization method called the maximum cross-swapping algorithm (MCA) to enhance the effective rank of the MIMO channel for achievable rate improvement. Numerical simulations are conducted to verify the effectiveness of RIS in improving the effective rank and the achievable rate. Moreover, we set up an RIS-assisted 2×2 MIMO communication prototype to validate the performance of our proposed algorithm through experimental measurements. The results show that compared to the MIMO channel without RIS, the RIS-assisted MIMO channel, optimized using the MCA, achieves a notable increase of 30.1% in the effective rank and 13.6% improvement in the achievable rate.

II. SYSTEM MODEL

We consider an RIS-assisted MIMO communication system as shown in Fig.1. The transmitter and the receiver have L and Q antennas, respectively. The RIS consists of N unit cells. The entire MIMO channel between the transmitter and the receiver

is comprised of the RIS-assisted channel and the non-RIS-assisted channel [3], [11], which can be modeled as

$$\mathbf{H} = \sqrt{\alpha} \underbrace{\mathbf{H}_{\text{rx}}^{\text{ris}} \mathbf{\Gamma} \mathbf{H}_{\text{ris}}^{\text{tx}}}_{\text{RIS-assisted channel}} + \sqrt{1-\alpha} \left(\underbrace{\sqrt{\frac{K}{1+K}} \mathbf{H}_{\text{LoS}} + \sqrt{\frac{1}{1+K}} \mathbf{H}_{\text{NLoS}}}_{\text{non-RIS-assisted channel}} \right), \quad (1)$$

where $\mathbf{H}_{\text{ris}}^{\text{tx}} \in \mathbb{C}^{N \times L}$ and $\mathbf{H}_{\text{rx}}^{\text{ris}} \in \mathbb{C}^{Q \times N}$ represent the channel between the transmitter and the RIS, and the channel between the RIS and the receiver, respectively. $\mathbf{\Gamma} \in \mathbb{C}^{N \times N}$ is a diagonal matrix composed of the reflection coefficients of each unit cell. $\mathbf{H}_{\text{LoS}} \in \mathbb{C}^{Q \times L}$ and $\mathbf{H}_{\text{NLoS}} \in \mathbb{C}^{Q \times L}$ represent the non-RIS-assisted line of sight (LoS) and non-LoS (NLoS) paths between the transmitter and the receiver, respectively. $\alpha \in (0, 1)$ denotes the power ratio of the RIS-assisted channel, i.e., the power ratio of $\mathbf{H}_{\text{rx}}^{\text{ris}} \mathbf{\Gamma} \mathbf{H}_{\text{ris}}^{\text{tx}}$ in the overall channel \mathbf{H} . K is the Rician factor of the non-RIS-assisted channel.

Specifically, the channel between the transmitter and the RIS can be expressed as

$$\mathbf{H}_{\text{ris}}^{\text{tx}} = \begin{bmatrix} h_{1,\text{ris}}^{1,\text{tx}} & h_{1,\text{ris}}^{2,\text{tx}} & \cdots & h_{1,\text{ris}}^{L,\text{tx}} \\ h_{2,\text{ris}}^{1,\text{tx}} & h_{2,\text{ris}}^{2,\text{tx}} & \cdots & h_{2,\text{ris}}^{L,\text{tx}} \\ \vdots & \vdots & \ddots & \vdots \\ h_{N,\text{ris}}^{1,\text{tx}} & h_{N,\text{ris}}^{2,\text{tx}} & \cdots & h_{N,\text{ris}}^{L,\text{tx}} \end{bmatrix}, \quad (2)$$

where $h_{n,\text{ris}}^{l,\text{tx}}$ is the channel coefficient between the l_{th} ($l = 0, 1, \dots, L$) transmit antenna and the n_{th} ($n = 0, 1, \dots, N$) unit cell U_n . Considering the wireless signal propagation loss between them, the channel coefficient can be modeled as [12]

$$h_{n,\text{ris}}^{l,\text{tx}} = \sqrt{\frac{G_{\text{tx}} F(\theta_n^{l,\text{AoA}}, \varphi_n^{l,\text{AoA}}) d_x d_z}{4\pi (d_{n,\text{ris}}^{l,\text{tx}})^2}} \times e^{-j2\pi d_{n,\text{ris}}^{l,\text{tx}}/\lambda}, \quad (3)$$

where G_{tx} denotes the gain of each transmit antenna, $\theta_n^{l,\text{AoA}}$ and $\varphi_n^{l,\text{AoA}}$ denote the angle of arrival (AoA) from the l_{th} transmit antenna to the unit cell U_n . $F(\theta, \varphi)$ is the normalized power radiation pattern of each unit cell [13], [14]. d_x and d_z denote the width and length of each unit cell, respectively. $d_{n,\text{ris}}^{l,\text{tx}}$ denotes the distance between the l_{th} transmit antenna and the unit cell U_n , and λ represents the wavelength. In analogy with $\mathbf{H}_{\text{ris}}^{\text{tx}}$, $\mathbf{H}_{\text{rx}}^{\text{ris}}$ can be modeled.

Furthermore, the reflection matrix of the RIS $\mathbf{\Gamma}$ can be represented as

$$\mathbf{\Gamma} = \text{diag} \{ e^{j\phi_1}, e^{j\phi_2}, \dots, e^{j\phi_N} \}, \quad (4)$$

where $e^{j\phi_n}$ denotes the reflection coefficient of unit cell U_n . In practice, continuous control of the reflection phase for each unit cell incurs significant hardware implementation costs. Thus, we consider the discrete implementation, where the reflection phase is taken only from a finite number of discrete values. We assign $\boldsymbol{\phi} = [\phi_1, \phi_2, \dots, \phi_N]$ to be the phase configuration vector of the RIS, satisfying $\forall \phi_n \in \Xi_b = \left\{ 0, \frac{2\pi}{2^b}, \dots, \frac{2\pi(2^b-1)}{2^b} \right\}$, where b denotes quantization bit of reflection phase of each unit cell.

As to the non-RIS-assisted channel, the LoS path between the transmitter and the receiver can be modeled as

$$\mathbf{H}_{\text{LoS}} = \begin{bmatrix} h_{1,\text{rx}}^{1,\text{tx}} & h_{1,\text{rx}}^{2,\text{tx}} & \cdots & h_{1,\text{rx}}^{L,\text{tx}} \\ h_{2,\text{rx}}^{1,\text{tx}} & h_{2,\text{rx}}^{2,\text{tx}} & \cdots & h_{2,\text{rx}}^{L,\text{tx}} \\ \vdots & \vdots & \ddots & \vdots \\ h_{Q,\text{rx}}^{1,\text{tx}} & h_{Q,\text{rx}}^{2,\text{tx}} & \cdots & h_{Q,\text{rx}}^{L,\text{tx}} \end{bmatrix}, \quad (5)$$

where $h_{q,\text{rx}}^{l,\text{tx}} = \sqrt{G_{\text{tx}} G_{\text{rx}} \lambda} / (4\pi d_{q,\text{rx}}^{l,\text{tx}}) \times e^{-j2\pi d_{q,\text{rx}}^{l,\text{tx}}/\lambda}$ denotes the channel coefficient of the LoS path between the l_{th} transmit antenna and the q_{th} ($q = 0, 1, \dots, Q$) receive antenna, $d_{q,\text{rx}}^{l,\text{tx}}$ and G_{rx} are the distance between them and the gain of each receive antenna, respectively. In addition, the NLoS path can be represented by

$$\mathbf{H}_{\text{NLoS}} = \frac{\sqrt{G_{\text{tx}} G_{\text{rx}} \lambda}}{4\pi d_{\text{rx}}^{\text{tx}}} \tilde{\mathbf{H}}_{\text{NLoS}}, \quad (6)$$

where $d_{\text{rx}}^{\text{tx}}$ is the distance between the center of the transmitter and the center of the receiver, and $\tilde{\mathbf{H}}_{\text{NLoS}} \in \mathbb{C}^{L \times Q}$ is the NLoS component. Each element of $\tilde{\mathbf{H}}_{\text{NLoS}}$ is an i.i.d. complex Gaussian random variable with zero mean and unit variance.

III. OPTIMIZATION METHOD

In this section, we introduce an optimization method to improve the MIMO channel. The effective rank is used as a metric to evaluate the orthogonality among the MIMO subchannels [11]. According to the definition in [10], the effective rank of the MIMO channel \mathbf{H} between the transmitter and the receiver can be expressed as

$$\text{erank}(\mathbf{H}) = \exp \left(\sum_{i=1}^{\text{rank}(\mathbf{H})} -\sigma'_i \ln \sigma'_i \right), \quad (7)$$

where $\text{rank}(\mathbf{H})$ is the rank of the MIMO channel, and $\sigma'_i = \sigma_i / \sum_i \sigma_i$ is the normalized singular value.

By incorporating RIS as a component of the MIMO channel, it is possible to optimize the configuration of the RIS $\boldsymbol{\phi}$ to improve the effective rank of the MIMO channel \mathbf{H} , thus improving the orthogonality of the subchannels and overall system performance. Hence, the optimization goal can be written as

$$\begin{aligned} & \underset{\boldsymbol{\phi}}{\text{maximize}} \text{erank}(\mathbf{H}) \\ & \text{subject to } \forall \phi_n \in \Xi_b, n = 1, 2, \dots, N. \end{aligned} \quad (8)$$

We propose an efficient optimization method named MCA to optimize the phase configuration of the RIS, which is described as follows.

1) *Iterating through random configurations*: In the MCA, we first generate a set of T random RIS phase configurations, i.e., $\Psi = \{\boldsymbol{\phi}_1, \dots, \boldsymbol{\phi}_T\}$. Then, we configure the RIS according to these T random configurations and obtain the corresponding effective rank of the MIMO channel \mathbf{H} . Furthermore, the T random RIS configurations are sorted in ascending order based on their individual effective ranks, and the top two configurations are selected as the parent set Ψ_{parent} to generate a new set of RIS phase configurations for the next round. The corresponding parent set is expressed as

$$\Psi_{\text{parent}} = \{\phi_{\text{max}}, \phi_{\text{submax}}\}, \quad (9)$$

where ϕ_{max} and ϕ_{submax} represent the RIS configuration with the highest and second-highest effective rank of the corresponding MIMO channel \mathbf{H} in the set Ψ , respectively.

2) *Cross-swapping the parent configurations*: We generate offspring RIS phase configurations denoted as $\Psi_{\text{son}} = \{\phi_1^{\text{son}}, \phi_2^{\text{son}}, \dots, \phi_{2^{N_{\text{new}}}}^{\text{son}}\}$ by sequentially cross-swapping the phase designs of the first N_{new} unit cells from the parent configurations $\{\phi_{\text{max}}, \phi_{\text{submax}}\}$. The detailed procedure is outlined in Method 1.

Method 1 Cross-swapping Parent Configurations to Generate Offspring Configurations.

```

1: input :  $N_{\text{new}}, \phi_{\text{max}}, \phi_{\text{submax}}$ 
2: for  $i = 1, 2, \dots, 2^{N_{\text{new}}}$  do
3:   convert  $i$  to a binary number  $i_b$  with  $N_{\text{new}}$  bits
4:   for  $j = 1, 2, \dots, N_{\text{new}}$  do
5:     if the  $j$ th bit of  $i_b$  equals to 0
6:       assign the  $j$ th element of  $\phi_{\text{max}}$  to the  $j$ th
       element of  $\phi_i^{\text{son}}$ 
7:     else if the  $j$ th bit of  $i_b$  equals to 1
8:       assign the  $j$ th element of  $\phi_{\text{submax}}$  to the  $j$ th
       element of  $\phi_i^{\text{son}}$ 
9:     end if
10:    assign the remaining elements of  $\phi_{\text{max}}$  to the
    remaining elements of  $\phi_i^{\text{son}}$ 
11:   end for
12: end for
13: output : offspring RIS configuration set  $\Psi_{\text{son}} =$ 
     $\{\phi_1^{\text{son}}, \phi_2^{\text{son}}, \dots, \phi_{2^{N_{\text{new}}}}^{\text{son}}\}$ 

```

3) *Obtaining the optimal offspring configuration*: After applying each newly generated offspring configuration to the RIS, we can calculate the corresponding effective rank of the MIMO channel \mathbf{H} . The optimal offspring configuration, denoted as ϕ_{mca} , is determined as the one with the highest effective rank among the set Ψ_{son} . The whole process of the MCA is summarized in Algorithm 1.

IV. NUMERICAL SIMULATION

In this section, we evaluate the performance improvement of the RIS-assisted MIMO channel through numerical simulations, utilizing the proposed optimization method. As illustrated in Fig. 2, we consider the column-controlled RIS, which can be treated as a uniform linear array (ULA). We set the centers of the transmit antennas, the receive antennas, and the RIS all positioned at the same height, thus reducing the system to two-dimension. The AoA φ_n^{AoA} and AoD φ_q^{AoD} are fixed at π and 0 in the x-y plane, respectively. In addition, $d_{\text{ris},x}^{\text{tx}}$ ($d_{\text{rx},x}^{\text{ris}}$) and $d_{\text{ris},y}^{\text{tx}}$ ($d_{\text{rx},y}^{\text{ris}}$) represent the corresponding distance between the center of the transmitter (receiver) and the center of the RIS in the x or y direction, respectively. These distances are illustrated in Table I. Moreover, d_{tx} and d_{rx} denote the transmit antenna spacing and the receive antenna spacing, respectively. When the transmit antennas and receive antennas are fixed, we can calculate $d_{n,\text{ris}}^{\text{tx}}$, $d_{q,\text{rx}}^{\text{ris}}$, $d_{q,\text{rx}}^{\text{tx}}$, $d_{\text{rx}}^{\text{tx}}$, θ_n^{AoA} , and θ_q^{AoD} based on the geometric relationship.

Algorithm 1 Maximum Cross-swapping Algorithm (MCA).

```

1: input :  $N, T, N_{\text{new}}, b$ 
2: generate a set  $\Psi$  containing  $T$  random RIS configurations
    $\{\phi_t\}_{t=1}^T$  based on  $\Xi_b$ 
3: calculate the effective rank of the MIMO channel  $\mathbf{H}$  with
   the RIS configured by each configuration  $\phi_t$ 
4: find the RIS configuration  $\phi_{\text{max}}$  and  $\phi_{\text{submax}}$  with the
   highest and second-highest effective rank of the corre-
   sponding MIMO channel  $\mathbf{H}$  in the set  $\Psi$ , respectively.

5: generate offspring RIS configuration set  $\Psi_{\text{son}}$  according to
   Method 1
6: for  $i = 1, 2, \dots, 2^{N_{\text{new}}}$  do
7:   calculate the corresponding effective rank of the
   MIMO channel  $\mathbf{H}$  with the RIS configured by  $\phi_i^{\text{son}}$ 
8: end for
9: output :  $\phi_{\text{mca}} = \arg \max_{\phi \in \Psi_{\text{son}}} \text{erank}(\mathbf{H})$ 

```

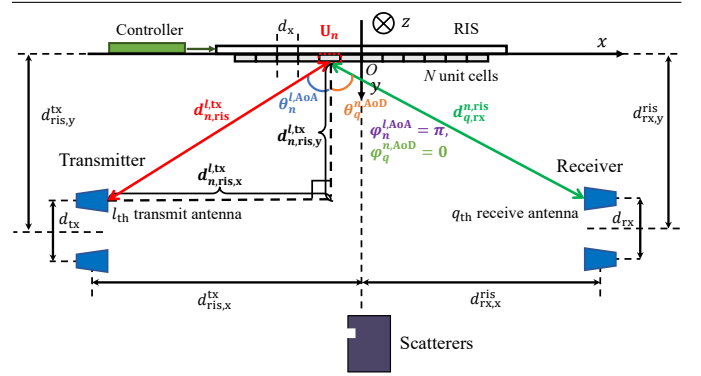


Fig. 2. Deployment of the considered RIS-assisted 2×2 MIMO communication system (top view).

The system operates at $f = 2.7$ GHz. Each column of the RIS can be seen as a macro unit cell, whose width and length are $d_x = 0.05$ m and $d_z = 1.6$ m, respectively. As shown in Fig. 2, the transmitter and receiver are both equipped with 2 antennas, that is $L = Q = 2$, with a transmit and receive gain being $G_{\text{tx}} = G_{\text{rx}} = 6$ dB. More specific system parameters are listed in Table I.

When zero-forcing (ZF) equalization is applied to recover the data streams, the achievable system rate can be expressed as [15]

$$R_{\text{ZF}}(\mathbf{H}, \rho) = \sum_{i=1}^{\text{rank}(\mathbf{H})} \log_2 \left(1 + \frac{\rho}{[(\mathbf{H}^H \mathbf{H})^{-1}]_{ii}} \right), \quad (10)$$

where ρ is the transmit signal-to-noise ratio (SNR) and $[\cdot]_{ii}$ denotes the i th diagonal element of a matrix. In the high SNR regime where water filling power allocation reduces to equal power allocation, the capacity of the MIMO channel, which is introduced as the upper bound of the simulation, can be approximated by [16]

$$C(\mathbf{H}, \rho) = \sum_{i=1}^{\text{rank}(\mathbf{H})} \log_2(1 + \sigma_i^2 \rho). \quad (11)$$

In the following simulated cases, we set the transmit SNR $\rho = 50$ dB and Rician factor $K = 20$ dB. All the results

TABLE I
PARAMETERS FOR THE NUMERICAL SIMULATION

RIS Parameters	Operating Frequency f	2.7 GHz
	Coding Type	1-bit phase
	Macro Unit Cell Number N	16/32/64
	Macro Unit Cell Width d_x	0.05 m
	Macro Unit Cell Length d_z	1.6 m
Distance Parameters	Transmitter to RIS $d_{\text{ris},y}^{\text{tx}}, d_{\text{ris},x}^{\text{tx}}$	1 m, 0.5 m
	RIS to Receiver $d_{\text{ris},y}^{\text{rx}}, d_{\text{ris},x}^{\text{rx}}$	1 m, 0.5 m
	Transmit Antenna Spacing d_{tx}	0.1 m
	Receive Antenna Spacing d_{rx}	0.1 m

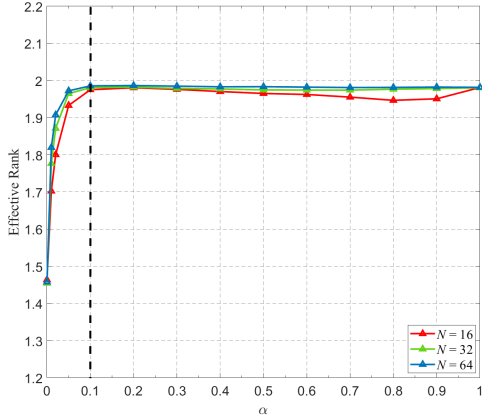


Fig. 3. Effective rank versus power ratio of the RIS-assisted channel for different numbers of unit cells.

are averaged over 1000 Monte Carlo channel realizations. We perform the MCA with $T = 160$ and $N_{\text{new}} = 4$.

Fig. 3 demonstrates the effective rank versus power ratio of the RIS-assisted channel for different numbers of unit cells. When the power ratio $\alpha = 0$, the MIMO channel \mathbf{H} is only composed of the non-RIS-assisted channel, and the corresponding effective rank is 1.46. The reason for the deficient effective rank is the lack of rich scattering in the propagation environment between the transmitter and receiver. As α increases, the corresponding power ratio of the RIS-assisted channel $\mathbf{H}_{\text{ris}}^{\text{ris}} \mathbf{\Gamma} \mathbf{H}_{\text{ris}}^{\text{tx}}$ in the MIMO channel \mathbf{H} rises. Consequently, the effective rank of \mathbf{H} rapidly approaches 2. The introduction of the RIS enhances the scattering environment. This result reveals leveraging the RIS can improve the effective rank of the MIMO channel.

We also evaluate the achievable rate of the ZF receiver and compare it with the upper bound as α increases, while considering varying numbers of unit cells. As shown in Fig. 4, when $N = 16$, the achievable rate of the ZF receiver increases first and then decreases. The upward trend is attributed to the improvement of the effective rank of MIMO channel \mathbf{H} . The subsequent downward trend occurs due to the limited number of unit cells, as the gain provided by the RIS-assisted channel is insufficient to compensate for the losses in the non-RIS-assisted channel. Thus, when power ratio α of the RIS-assisted channel $\mathbf{H}_{\text{ris}}^{\text{ris}} \mathbf{\Gamma} \mathbf{H}_{\text{ris}}^{\text{tx}}$ in the channel \mathbf{H} increases, the corresponding achievable rate actually decreases. However, when the RIS consists of more unit cells, i.e., $N = 32$ or 64 , the RIS-assisted channel has higher gains. As a result, the achievable rate of the ZF receiver continues to increase. Increasing N enhances the achievable rate of the ZF receiver. This effect becomes more pronounced with larger α .

Additionally, it can be observed that as the power ratio α

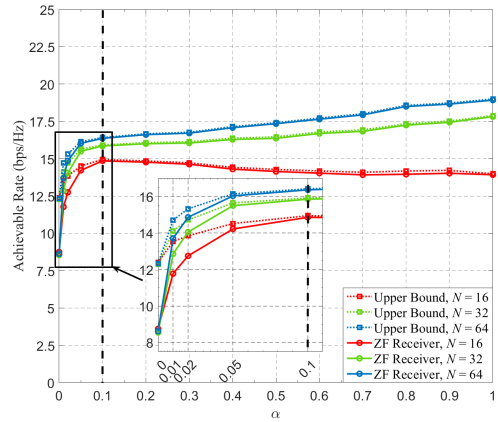


Fig. 4. Comparison of the achievable rate for the ZF receiver and the upper bound with increasing α when considering different numbers of unit cells.

increases, the effective rank of the 2×2 MIMO channel \mathbf{H} approaches the upper limit of 2 in the right region indicated by the black dashed line in Fig. 3. This result implies that the two subchannels of \mathbf{H} are orthogonal to each other. Meanwhile, the achievable rate of the simple ZF receiver approaches the upper bound, as shown in Fig. 4. Leveraging the RIS to optimize the effective rank of the MIMO channel, we can enhance the MIMO channel itself, simplify the receiver algorithm, and ultimately improve the overall performance of the system.

V. EXPERIMENTAL MEASUREMENT

In this section, we set up an RIS-assisted 2×2 MIMO communication prototype to conduct experimental measurements. As depicted in Fig. 5, the transmitter and the receiver consist of two antennas and the software defined radio (SDR) platform, respectively. The RIS is placed aside, with its center aligned with the center of all antennas at the same height, thereby establishing an RIS-assisted 2×2 MIMO communication system. The parameters of the fabricated RIS and the corresponding distances are identical to those utilized in the numerical simulation.

When the configuration of RIS is completed, the receiver uses the least squares (LS) method to estimate the overall MIMO channel $\hat{\mathbf{H}}$. Subsequently, the corresponding effective rank of the channel is calculated based on equation (7) as a metric for the MCA to optimize the RIS configuration. The achievable rate of the ZF receiver can be obtained by summing up the achievable rates of each independent data stream after ZF equalization, which can be expressed as

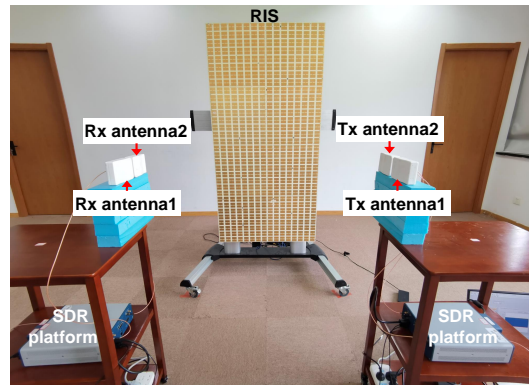


Fig. 5. A photo of the RIS-assisted 2×2 MIMO communication prototype.

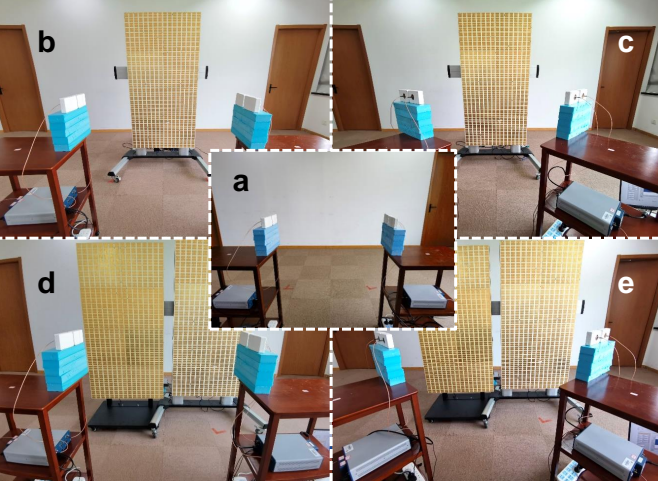


Fig. 6. Layout of experimental scenarios: (a) Transmitter faces receiver without RIS, (b) Transmitter faces receiver with one RIS aside, (c) Transmitter and receiver both face one RIS, (d) Transmitter faces receiver with two RISs aside, (e) Transmitter and receiver both face two RISs.

$$R_{ZF}^{\text{mea}}(\mathbf{H}, \rho_i^{\text{ZF}}) = \sum_{i=1}^{\text{rank}(\mathbf{H})} \log_2(1 + \rho_i^{\text{ZF}}), \quad (12)$$

where ρ_i^{ZF} is the SNR of the i_{th} data stream after ZF equalization. The specific measurement method for each SNR ρ_i^{ZF} can be found in Sections IV-D and V-B of reference [12].

In order to modify the power ratio α of the RIS-assisted channel $\mathbf{H}_{\text{rx}}^{\text{ris}} \mathbf{\Gamma} \mathbf{H}_{\text{ris}}^{\text{tx}}$ in the MIMO channel \mathbf{H} , we alter the orientation of the antennas towards the RISs. As depicted in Fig. 6(a), when the transmitter directly faces the receiver without any RIS, the corresponding α value is 0. In Fig. 6(b) and Fig. 6(d), where the transmitter faces the receiver with the RISs placed aside, the corresponding α slightly exceeds 0. As shown in Fig. 6(c) and Fig. 6(e), when both the transmitter and the receiver face the RISs, the corresponding α approaches 1. Furthermore, we evaluated the impact of increasing the number of unit cells by comparing the results obtained with one RIS and two RISs. Table II summarizes the corresponding measurement results.

It can be observed that when using one RIS ($N = 16$), the achievable rate of the ZF receiver R_{ZF}^{mea} increases from 17.7 to 19.4 bps/Hz at the beginning and then decreases to 18.9 bps/Hz as α increases. Meanwhile, the effective rank rises from 1.53 to 1.96. However, when using two RISs ($N = 32$), R_{ZF}^{mea} continuously increases by 13.6%, from 17.7 to 20.1 bps/Hz as α increases. Simultaneously, the effective rank rises from 1.53 to 1.96, obtaining a 30.1% increase. In scenarios where the RIS-assisted channel dominates \mathbf{H} , as depicted in Fig. 6(c) and Fig. 6(e), adding one RIS (increasing N from 16 to 32) leads to a 1.2 bps/Hz increase in R_{ZF}^{mea} . The measurement results are consistent with the simulation results and verify that RIS can be effectively used to optimize the effective rank of the channel and improve the system performance.

VI. CONCLUSION

In this study, we proposed an efficient RIS optimization method to enhance the effective rank of the MIMO channel for achievable rate improvement in RIS-assisted systems. Through

TABLE II
RESULTS OF THE EXPERIMENTAL MEASUREMENT

No.	α and N	$\text{erank}(\mathbf{H})$	ρ_1^{ZF} (dB)	ρ_2^{ZF} (dB)	R_{ZF}^{mea} (bps/Hz)
a	$\alpha = 0$	1.53	26.6	27.1	17.7
b	α slightly exceed 0 $N = 16$	1.70	27.9	30.2	19.4
c	α approaches 1 $N = 16$	1.96	28.1	28.8	18.9
d	α slightly exceed 0 $N = 32$	1.65	28.1	29.5	19.2
e	α approaches 1 $N = 32$	1.99	30.2	30.4	20.1

numerical simulations and experimental measurements, we have confirmed that RISs can be utilized to improve the effective rank of the MIMO channel as well as the achievable rate effectively. The results show that the RIS-assisted MIMO channel optimized using MCA, compared to the scenario without RIS, exhibited an increase of 30.1% in effective rank and a 13.6% achievable rate improvement. Based on these promising findings, our study reveals the superior performance of RIS in optimizing MIMO channels, which highlights the potential applications of RISs in future networks.

REFERENCES

- [1] T. J. Cui, M. Q. Qi, X. Wan, J. Zhao, and Q. Cheng, "Coding metamaterials, digital metamaterials and programmable metamaterials," *Light: Sci. Appl.*, vol. 3, no. 10, p. e218, Oct. 2014.
- [2] M. Di Renzo *et al.*, "Smart radio environments empowered by reconfigurable intelligent surfaces: How it works, state of research, and the road ahead," *IEEE J. Select. Areas Commun.*, vol. 38, no. 11, pp. 2450-2525, Nov. 2020.
- [3] Y. Han, W. Tang, S. Jin, C.-K. Wen, and X. Ma, "Large intelligent surface-assisted wireless communication exploiting statistical CSI," *IEEE Trans. Veh. Technol.*, vol. 68, no. 8, pp. 8238-8242, Aug. 2019.
- [4] J. Sang *et al.*, "Coverage enhancement by deploying RIS in 5G commercial mobile networks: Field trials," *IEEE Wireless Commun.*, early access, Dec. 2022.
- [5] S. Meng *et al.*, "An efficient multi-beam generation method for millimeter-wave reconfigurable intelligent surface: Simulation and measurement," *IEEE Trans. Veh. Technol.*, early access, May 2023.
- [6] W. Chen, C.-K. Wen, X. Li, M. Matthaiou, and S. Jin, "Channel customization for limited feedback in RIS-assisted FDD systems," *IEEE Trans. Wireless Commun.*, vol. 22, no. 7, pp. 4505-4519, Jul. 2023.
- [7] R. Li *et al.*, "Ergodic achievable rate analysis and optimization of RIS-assisted millimeter-wave MIMO communication systems," *IEEE Trans. Wireless Commun.*, vol. 22, no. 2, pp. 972-985, Feb. 2023.
- [8] N. S. Perovic *et al.*, "Achievable rate optimization for MIMO systems with reconfigurable intelligent surfaces," *IEEE Trans. Wireless Commun.*, vol. 20, no. 6, pp. 3865-3882, Jun. 2021.
- [9] W. Chen, C.-K. Wen, X. Li, and S. Jin, "Channel customization for joint Tx-RISs-Rx design in hybrid mmWave systems," *IEEE Trans. Wireless Commun.*, early access, Apr. 2023.
- [10] O. Roy and M. Vetterli, "The effective rank: A measure of effective dimensionality," in *Proc. 15th Eur. Signal Process. Conf. (EUSIPCO)*, Sep. 2007, pp. 606-610.
- [11] M. A. ElMossallamy *et al.*, "On spatial multiplexing using reconfigurable intelligent surfaces," *IEEE Wirel. Commun. Lett.*, vol. 10, no. 2, pp. 226-230, Feb. 2021.
- [12] W. Tang *et al.*, "MIMO transmission through reconfigurable intelligent surface: System design, analysis, and implementation," *IEEE J. Select. Areas Commun.*, vol. 38, no. 11, pp. 2683-2699, Nov. 2020.
- [13] W. Tang *et al.*, "Path loss modeling and measurements for reconfigurable intelligent surfaces in the millimeter-wave frequency band," *IEEE Trans. Commun.*, vol. 70, no. 9, pp. 6259-6276, Sep. 2022.
- [14] W. Tang *et al.*, "Wireless communications with reconfigurable intelligent surface: Path loss modeling and experimental measurement," *IEEE Trans. Wireless Commun.*, vol. 20, no. 1, pp. 421-439, Jan. 2021.
- [15] M. Matthaiou, C. Zhong, and T. Ratnarajah, "Novel generic bounds on the sum rate of MIMO ZF receivers," *IEEE Trans. Signal Process.*, vol. 59, no. 9, pp. 4341-4353, Sep. 2011.
- [16] A. Goldsmith, *Wireless Communications*. Cambridge, U.K.: Cambridge Univ. Press, 2005.